

---

A mixed finite element formulation for generalised  
Newtonian fluid flows with appropriate natural outflow  
boundary conditions

D. Pacheco, T. Müller, O. Steinbach, G. Brenn

---

**Berichte aus dem  
Institut für Angewandte Mathematik**



# Technische Universität Graz

---

A mixed finite element formulation for generalised  
Newtonian fluid flows with appropriate natural outflow  
boundary conditions

D. Pacheco, T. Müller, O. Steinbach, G. Brenn

---

**Berichte aus dem  
Institut für Angewandte Mathematik**

Bericht 2020/1

Technische Universität Graz  
Institut für Angewandte Mathematik  
Steyrergasse 30  
A 8010 Graz

**WWW:** <http://www.applied.math.tugraz.at>

© Alle Rechte vorbehalten. Nachdruck nur mit Genehmigung des Autors.

# A mixed finite element formulation for generalised Newtonian fluid flows with appropriate natural outflow boundary conditions

Douglas R. Q. Pacheco <sup>1</sup>, Thomas S. Müller <sup>2</sup>, Olaf Steinbach <sup>3</sup> and Günter Brenn <sup>4</sup>

<sup>1,3</sup> Institute of Applied Mathematics, Graz University of Technology, Graz, Austria

<sup>2,4</sup> Institute of Fluid Mechanics and Heat Transfer, Graz University of Technology, Graz, Austria

<sup>1,2,3,4</sup> Graz Center of Computational Engineering, Graz University of Technology, Graz, Austria

---

## Abstract

The matter of appropriate boundary conditions for open or truncated outflow regions was for a long time focus of intense discussion in the computational fluid dynamics community. In the context of finite element methods, it is widely acknowledged that the “do-nothing” natural boundary condition from the Laplace formulation of the Navier-Stokes system yields accurate, physically consistent solutions. Nevertheless, when the viscosity is no longer a constant, as in generalised Newtonian fluids, the use of the classical Laplace formulation is not possible anymore. Thus, it is common practice to use the so-called stress-divergence formulation with natural boundary conditions that are known to cause unphysical behaviour close to the outlet. In order to overcome such issues, this work presents a novel mixed variational formulation – and corresponding finite element method – that can be seen as a generalisation of the Navier-Stokes Laplace formulation to fluids with flow field-dependent viscosity. By appropriately manipulating the viscous terms in the variational formulation and employing a simple projection of the constitutive law, it is possible to devise a formulation with the desired natural boundary conditions and low computational complexity. Several numerical examples are presented to showcase the potential of this novel method.

---

## 1. Introduction

In various incompressible flow applications, it is often necessary to cut the spatial domain due to computational limitations. For instance, when simulating the blood flow in an artery, as it is not viable to consider the whole circulatory system, a truncated computational domain containing only the region of interest must be considered. From that arises the need to specify appropriate boundary conditions at the open outlet (i.e., where the “cut” was made). Since no *a priori* flow data is normally available at outlets, it is crucial to apply boundary conditions that retain the correct physical behaviour – or

---

<sup>1</sup>Email address: pacheco@math.tugraz.at, corresponding author

at least minimise the upstream effect of the truncation. In that context, several variational formulations can be distinguished for the incompressible Navier-Stokes equations, depending on how the viscous and convective terms are handled [1]. The most popular treatments of the viscous stress are the Laplace formulation and the stress-divergence form. The former is computationally cheaper and simpler [2], whereas the latter can be applied straightforwardly to more general (e.g., non-Newtonian) fluids [3]. Although completely equivalent in the Dirichlet case, they can yield different solutions when natural boundary conditions are considered [4]. In the stress-divergence formulation, assuming zero natural outflow data is known for generating unphysical flow behaviour that can have a considerable upstream effect, and for that reason the Laplace formulation is preferred when possible [5].

For generalised Newtonian fluids, however, the presence of flow-dependent viscosity prohibits the use of the simple Laplace form for the viscous term. Therefore, it is common practice to use the stress-divergence formulation and, if necessary, extend the computational domain artificially in order to keep the unphysical outflow behaviour distant from the region of interest [6]. To overcome such limitations, the present work aims at the design of a suitable finite element framework for generalised Newtonian fluids, yielding appropriate natural outflow boundary conditions. This is done through the derivation of a mixed finite element method (FEM) that can be seen as a generalisation of the Laplace formulation to the case of fluids with variable viscosity. Numerical examples considering various fluid models showcase the potential of this novel formulation to attain accurate solutions for problems with open boundaries.

## 2. Variational formulations

In what follows, three variational formulations are discussed: first, the stress-divergence one, which is popular for generalised Newtonian fluids (while perhaps not so much for the Newtonian case), then the classical Laplace formulation for Newtonian fluids, and finally a novel formulation that generalises the Laplace form to variable viscosity cases. For simplicity of presentation, only the stationary problem is tackled herein, but no modifications are required for the time-dependent case.

The balance of linear momentum for a stationary flow can be stated as

$$(\rho \nabla \mathbf{u}) \mathbf{u} - \nabla \cdot \mathbb{T} = \rho \mathbf{g}, \quad (1)$$

where  $\mathbf{u}$  is the flow velocity,  $\mathbb{T}$  is the Cauchy stress tensor,  $\mathbf{g}$  is a specific body force and  $\rho$  is the density. For concision, the body force  $\rho \mathbf{g}$  will be dropped. Note that the gradient of a vector  $\mathbf{u}$  is defined as the second-order tensor  $\nabla \mathbf{u}$ , in which

$$(\nabla \mathbf{u})_{ij} := \frac{\partial u_i}{\partial x_j}, \quad (2)$$

where  $u_i$  is the  $i$ -th component of  $\mathbf{u}$  and  $x_j$  is the  $j$ -th spatial coordinate. The conservation of mass for an incompressible flow is simply

$$\nabla \cdot \mathbf{u} = 0. \quad (3)$$

Consider a bounded Lipschitz domain  $\Omega \subset \mathbb{R}^d$ ,  $d = 2, 3$ . The boundary  $\Gamma := \partial\Omega$  is decomposed into two non-overlapping regions  $\Gamma_D$  and  $\Gamma_N$ . In  $\Gamma_D$  the velocities are prescribed:  $\mathbf{u}|_{\Gamma_D} = \mathbf{u}_D$ . The treatment of  $\Gamma_N$ , on the other hand, depends on the variational formulation employed for the momentum equation, as shown next.

### 2.1. Stress-divergence form

To devise a variational formulation, Eq. (1) is first multiplied by a test function  $\mathbf{w} \in [H^1(\Omega)]^d$ , with  $\mathbf{w}|_{\Gamma_D} = \mathbf{0}$ , and integrated over  $\Omega$ :

$$\int_{\Omega} [(\rho \nabla \mathbf{u}) \mathbf{u}] \cdot \mathbf{w} \, d\Omega - \int_{\Omega} (\nabla \cdot \mathbb{T}) \cdot \mathbf{w} \, d\Omega = 0. \quad (4)$$

Since  $\mathbb{T}$  in general depends on  $\nabla \mathbf{u}$ , integration by parts is applied to avoid second-order derivatives of  $\mathbf{u}$  in the formulation. This leads to the weak form

$$\int_{\Omega} [(\rho \nabla \mathbf{u}) \mathbf{u}] \cdot \mathbf{w} \, d\Omega + \int_{\Omega} \mathbb{T} : \nabla \mathbf{w} \, d\Omega = \int_{\Gamma_N} \mathbf{t} \cdot \mathbf{w} \, d\Gamma =: \langle \mathbf{t}, \mathbf{w} \rangle_{\Gamma_N}, \quad (5)$$

where  $\mathbf{t} := \mathbb{T} \mathbf{n}$  is the normal boundary traction and  $\mathbf{n}$  is the outward unit normal vector on  $\Gamma$ . This formulation is a very general one, since no conditions on the material behaviour have been assumed so far. Before introducing a material law, the Cauchy stress tensor  $\mathbb{T}$  is split into hydrostatic and deviatoric parts:

$$\mathbb{T} = -p \mathbb{I} + \mathbb{S}, \quad (6)$$

in which  $p$  is the pressure,  $\mathbb{I}$  is the  $d \times d$  identity tensor and  $\mathbb{S}$  is the deviatoric stress tensor. For a generalised Newtonian fluid, the stress-strain relationship is given by

$$\mathbb{S} = 2\mu \nabla^s \mathbf{u}, \quad (7)$$

where  $\mu$  is the dynamic viscosity, which in general depends on the symmetric part of the velocity gradient,  $\nabla^s \mathbf{u}$ , namely,

$$\nabla^s \mathbf{u} := \frac{1}{2} \left[ \nabla \mathbf{u} + (\nabla \mathbf{u})^\top \right]. \quad (8)$$

Substituting Eqs. (6) and (7) into the weak form (5) leads to the variational formulation: Find  $(\mathbf{u}, p) \in [H^1(\Omega)]^d \times L^2(\Omega)$ , with  $\mathbf{u}|_{\Gamma_D} = \mathbf{u}_D$ , such that for all  $(\mathbf{w}, q) \in [H^1(\Omega)]^d \times$

$L^2(\Omega)$ , with  $\mathbf{w}|_{\Gamma_D} = \mathbf{0}$ ,

$$c(\mathbf{u}, \mathbf{u}, \mathbf{w}) + a(\mathbf{u}, \mathbf{w}) - b(p, \mathbf{w}) = \langle \mathbf{t}, \mathbf{w} \rangle_{\Gamma_N}, \quad (9)$$

$$b(q, \mathbf{u}) = 0, \quad (10)$$

where  $\mathbf{t} = (-p\mathbb{I} + 2\mu\nabla^s\mathbf{u})\mathbf{n}$  and

$$c(\mathbf{u}, \mathbf{v}, \mathbf{w}) := \int_{\Omega} [(\rho\nabla\mathbf{v})\mathbf{u}] \cdot \mathbf{w} \, d\Omega, \quad (11)$$

$$a(\mathbf{u}, \mathbf{w}) := \int_{\Omega} 2\mu\nabla^s\mathbf{u} : \nabla^s\mathbf{w} \, d\Omega, \quad (12)$$

$$b(p, \mathbf{w}) := \int_{\Omega} (\nabla \cdot \mathbf{w}) p \, d\Omega. \quad (13)$$

If  $\mu$  depends on  $\nabla^s\mathbf{u}$ , the function that describes such dependence is introduced directly into the form  $a(\mathbf{u}, \mathbf{w})$ .

In this so-called stress-divergence formulation, the natural boundary condition is to prescribe normal boundary tractions  $\mathbf{t}$  on  $\Gamma_N$ . On an open outflow boundary, the usual approach is to “do nothing”, i.e., simply consider  $\mathbf{t} = \mathbf{0}$  and drop the boundary term. However, it is widely known that prescribing zero normal traction on a cut outflow boundary can lead to unphysical flow behaviour, even for the simplest case of laminar flow through a straight pipe [4]. Nonetheless, this is still the most popular approach in the non-Newtonian case (e.g., [6, 7, 8, 9, 10]). Then, what is often done is to extend the computational domain artificially to keep the spurious behaviour away from the region of interest.

## 2.2. Laplace form (Newtonian case)

For a Newtonian fluid, since the viscosity  $\mu$  is a constant, it is possible to simplify the viscous term as

$$\nabla \cdot (2\mu\nabla^s\mathbf{u}) = \mu\nabla \cdot (\nabla\mathbf{u}) + \mu\nabla \cdot [(\nabla\mathbf{u})^\top] = \mu\Delta\mathbf{u} + \mu\nabla(\nabla \cdot \mathbf{u}) = \mu\Delta\mathbf{u}, \quad (14)$$

since  $\nabla \cdot \mathbf{u} = 0$ . Now, as the term  $\nabla \cdot \mathbb{T}$  reduces to  $-\nabla p + \mu\Delta\mathbf{u}$ , integration by parts will lead to a viscous bilinear form and a natural boundary condition that are different from the stress-divergence case:

$$\int_{\Omega} [(\rho\nabla\mathbf{u})\mathbf{u}] \cdot \mathbf{w} \, d\Omega + \int_{\Omega} \mu\nabla\mathbf{u} : \nabla\mathbf{w} \, d\Omega - \int_{\Omega} p\nabla \cdot \mathbf{w} \, d\Omega = \int_{\Gamma_N} [(-p\mathbb{I} + \mu\nabla\mathbf{u})\mathbf{n}] \cdot \mathbf{w} \, d\Gamma. \quad (15)$$

In this Laplace formulation, the boundary term is no longer the normal traction  $\mathbf{t}$ , but instead a “pseudo-traction”  $\tilde{\mathbf{t}} = (-p\mathbb{I} + \mu\nabla\mathbf{u})\mathbf{n}$ . In fact, for this formulation, the “do-nothing” boundary condition ( $\tilde{\mathbf{t}} = \mathbf{0}$ ) on the outlet allows the flow to leave the computational domain “freely”, in the sense that it has minimal effect on the flow and allows



the use of truncated computational domains (excellent discussions and examples can be found in [1, 4, 11, 12]).

### 2.3. New formulation

In spite of the shortcomings of the stress-divergence formulation for problems with open boundaries, it can be readily applied to generalised Newtonian fluids, whereas the Laplace form is not possible when  $\mu = \mu(\nabla^s \mathbf{u})$ . Of course, it is possible to enforce the appropriate outflow condition ( $\tilde{\mathbf{t}} = \mathbf{0}$ ) in the stress-divergence formulation – despite not being the natural one – by adding appropriate boundary integrals to the weak form. However, for implementation-related reasons, the use of boundary operators is normally avoided in most finite element frameworks.

In this context, the motivation of the present work is to reformulate the variational problem for generalised Newtonian fluids so as to yield the same natural boundary conditions as in the Newtonian Laplace formulation – whilst maintaining simple implementation and low computational cost. The first step is to rewrite the viscous term as

$$\nabla \cdot (2\mu \nabla^s \mathbf{u}) = 2\nabla^s \mathbf{u} \nabla \mu + \mu \nabla \cdot (2\nabla^s \mathbf{u}) = 2\nabla^s \mathbf{u} \nabla \mu + \mu \Delta \mathbf{u} + \mu \nabla (\nabla \cdot \mathbf{u}) = 2\nabla^s \mathbf{u} \nabla \mu + \mu \Delta \mathbf{u}. \quad (16)$$

Hence, the viscous contribution in the variational formulation reads

$$- \int_{\Omega} (\nabla \mathbf{u} \nabla \mu) \cdot \mathbf{w} \, d\Omega - \int_{\Omega} [(\nabla \mathbf{u})^\top \nabla \mu] \cdot \mathbf{w} \, d\Omega - \int_{\Omega} (\mu \Delta \mathbf{u}) \cdot \mathbf{w} \, d\Omega. \quad (17)$$

As in the Newtonian case, the natural boundary condition is obtained through integration by parts of the terms containing the velocity Laplacian and the pressure gradient:

$$\int_{\Omega} \mathbf{w} \cdot (\nabla p - \mu \Delta \mathbf{u}) \, d\Omega = \int_{\Omega} \nabla \mathbf{u} : \nabla (\mu \mathbf{w}) \, d\Omega - \int_{\Omega} p \nabla \cdot \mathbf{w} \, d\Omega - \int_{\Gamma_N} \mathbf{w} \cdot [(-p\mathbb{I} + \mu \nabla \mathbf{u}) \mathbf{n}] \, d\Gamma, \quad (18)$$

where exactly the same natural boundary condition as in the Laplace formulation for Newtonian fluids can be identified. Moreover,

$$\int_{\Omega} \nabla \mathbf{u} : \nabla (\mu \mathbf{w}) \, d\Omega = \int_{\Omega} \nabla \mathbf{u} : (\mu \nabla \mathbf{w} + \mathbf{w} \otimes \nabla \mu) \, d\Omega = \int_{\Omega} \mu \nabla \mathbf{u} : \nabla \mathbf{w} + (\nabla \mathbf{u} \nabla \mu) \cdot \mathbf{w} \, d\Omega. \quad (19)$$

Since the second term in Eq. (19) and the first integral in Eq. (17) cancel out, the weak form of the momentum equation finally reduces to

$$\int_{\Omega} [(\rho \nabla \mathbf{u}) \mathbf{u}] \cdot \mathbf{w} \, d\Omega + \int_{\Omega} \mu \nabla \mathbf{u} : \nabla \mathbf{w} \, d\Omega - \int_{\Omega} [(\nabla \mathbf{u})^\top \nabla \mu] \cdot \mathbf{w} \, d\Omega - \int_{\Omega} p \nabla \cdot \mathbf{w} \, d\Omega = \int_{\Gamma_N} \tilde{\mathbf{t}} \cdot \mathbf{w} \, d\Gamma. \quad (20)$$

Note that, if  $\mu$  is a constant, the integral containing  $\nabla \mu$  vanishes and the Laplace form for Newtonian fluids is recovered.

At this point, there is one final issue to be addressed: the need to compute  $\nabla\mu$ . For a generalised Newtonian fluid, the viscosity is normally a function of  $\nabla^s\mathbf{u}$ . This means that the presence of  $\nabla\mu$  in the variational formulation would require second-order derivatives of the velocity field, which is prohibitive in the framework of classical  $C^0$  finite elements. However, a mixed approach can be employed to circumvent this issue. Instead of substituting the non-Newtonian law  $\mu = \mu(\nabla^s\mathbf{u})$  explicitly into the weak form, the idea is to introduce the viscosity as an independent unknown  $\tilde{\mu}$ , and recover it weakly through a continuous  $L^2$  projection. The mixed formulation then reads: Find  $(\mathbf{u}, p, \tilde{\mu}) \in [H^1(\Omega)]^d \times L^2(\Omega) \times H^1(\Omega)$ , with  $\mathbf{u}|_{\Gamma_D} = \mathbf{u}_D$ , such that for all  $(\mathbf{w}, q, r) \in [H^1(\Omega)]^d \times L^2(\Omega) \times L^2(\Omega)$ , with  $\mathbf{w}|_{\Gamma_D} = \mathbf{0}$ ,

$$c(\mathbf{u}, \mathbf{u}, \mathbf{w}) + l(\tilde{\mu}, \mathbf{u}, \mathbf{w}) - b(p, \mathbf{w}) = \langle \tilde{\mathbf{t}}, \mathbf{w} \rangle_{\Gamma_N}, \quad (21)$$

$$b(q, \mathbf{u}) = 0, \quad (22)$$

$$(\tilde{\mu}, r) = (\mu(\nabla^s\mathbf{u}), r), \quad (23)$$

with

$$l(\tilde{\mu}, \mathbf{u}, \mathbf{w}) := \int_{\Omega} \tilde{\mu} \nabla \mathbf{u} : \nabla \mathbf{w} \, d\Omega - \int_{\Omega} [(\nabla \mathbf{u})^\top \nabla \tilde{\mu}] \cdot \mathbf{w} \, d\Omega, \quad (24)$$

$$(\tilde{\mu}, r) := \int_{\Omega} \tilde{\mu} r \, d\Omega. \quad (25)$$

One then ends up with a nonlinear mixed formulation having velocity, pressure and viscosity as unknowns. Therefore, at the expense of one additional scalar unknown, it is possible to compute physically accurate solutions on truncated domains, as shown in Section 4.

### 3. Discretisation and solution

Let  $\psi_i^{\mathbf{u}}$ ,  $\psi_i^p$  and  $\psi_i^{\tilde{\mu}}$  denote the shape functions used for velocity, pressure and viscosity, respectively, at some mesh node  $i$ . In order to attain a stable formulation, Taylor-Hood elements are used for the velocity-pressure pair: second- and first-order polynomial interpolation for velocity and pressure, respectively. First-order interpolation is used for the viscosity.

A quick choice of iterative method to solve the present nonlinear problem would be Newton-Raphson. Yet, by naively doing so, one would spoil the simple coupling between velocity and viscosity on the projection step, thereby generating a fully-coupled system and increasing computational cost. Conversely, Picard-like methods are an attractive option here. In fact, an iterative method can be specifically devised so as to exploit the particular features of the nonlinear system at hand here. First, the following splitting is

considered for the viscous term:

$$l(\mu, \mathbf{u}, \mathbf{w}) = k(\mu, \mathbf{u}, \mathbf{w}) - s(\mu, \mathbf{u}, \mathbf{w}) = \int_{\Omega} \mu \nabla \mathbf{u} : \nabla \mathbf{w} \, d\Omega - \int_{\Omega} [(\nabla \mathbf{u}) \mathbf{w}] \cdot \nabla \mu \, d\Omega. \quad (26)$$

The form  $k$  is the usual weak Laplacian arising in the Navier-Stokes problem, and is normally incorporated into the velocity-velocity block of the system. The main question is then how to handle the additional part  $s$ , as it can be incorporated into either the velocity-velocity block or the velocity-viscosity block. The following approach is proposed: Given a previous iterate  $(\mathbf{u}^n, p^n, \tilde{\mu}^n)$ , the next iterate  $(\mathbf{u}^{n+1}, p^{n+1}, \tilde{\mu}^{n+1})$  is such that

$$(\tilde{\mu}^{n+1}, r) = (\mu(\nabla^s \mathbf{u}^n), r), \quad (27)$$

$$c(\mathbf{u}^{n+1}, \mathbf{u}^n, \mathbf{w}) + k(\tilde{\mu}^{n+1}, \mathbf{u}^{n+1}, \mathbf{w}) - b(p^{n+1}, \mathbf{w}) = s(\tilde{\mu}^{n+1}, \mathbf{u}^n, \mathbf{w}) + \langle \tilde{\mathbf{t}}, \mathbf{w} \rangle_{\Gamma_N}, \quad (28)$$

$$b(q, \mathbf{u}^{n+1}) = 0, \quad (29)$$

whose discrete counterpart is

$$\mathbf{M} \tilde{\underline{\mu}}^{n+1} = \underline{f}(\underline{\mathbf{u}}^n), \quad (30)$$

$$\begin{bmatrix} \mathbf{C}(\underline{\mathbf{u}}^n) + \mathbf{K}(\tilde{\underline{\mu}}^{n+1}) & -\mathbf{B}^\top \\ \mathbf{B} & \mathbf{0} \end{bmatrix} \begin{Bmatrix} \underline{\mathbf{u}}^{n+1} \\ \underline{p}^{n+1} \end{Bmatrix} = \begin{Bmatrix} \underline{\mathbf{b}} + \mathbf{S}(\underline{\mathbf{u}}^n) \tilde{\underline{\mu}}^{n+1} \\ \underline{0} \end{Bmatrix}, \quad (31)$$

where  $\mathbf{K}$ ,  $\mathbf{C}$  and  $\mathbf{B}$  are the usual stiffness, convection and divergence matrices from the Navier-Stokes problem (*c.f.* John [2]),  $\mathbf{M}$  is a standard mass matrix and  $\underline{\mathbf{b}}$  is a vector coming from the boundary conditions and/or body forces; matrix  $\mathbf{S}(\underline{\mathbf{u}})$  has  $d$  blocks with the following structure:

$$\mathbf{S} = \begin{bmatrix} \mathbf{S}^1 \\ \vdots \\ \mathbf{S}^d \end{bmatrix}, \quad \text{with } S_{ij}^k = \int_{\Omega} \frac{\partial \mathbf{u}}{\partial x_k} \cdot (\psi_i^{\mathbf{u}} \nabla \psi_j^{\tilde{\mu}}) \, d\Omega. \quad (32)$$

In this way, it is possible to recover the viscosity separately from the rest of the system, which keeps the computational overhead from introducing an additional unknown to a minimum. As a consequence, the additional viscous term introduced by the present formulation can be treated simply as a right-hand side instead of contributing to the coefficient matrix. Therefore, the system matrix left to be inverted in Eq. (31) is as in the classical Laplace formulation for Navier-Stokes, which allows a variety of well known efficient incompressible flow solvers and preconditioners to be readily applied here – at this stage, however, direct solvers are used. Then, a simple Aitken relaxation step is added after each iteration, which results in quadratic convergence for the overall iterative solver (refer to [13] for details).

## 4. Numerical examples

In this section, the method developed herein is tested for various benchmark problems. For simplicity, only the two-dimensional problem is tackled, with quadrilateral elements for the discretisation. The spatial coordinates  $x_1$  and  $x_2$  will be denoted by  $x$  and  $y$ , respectively, and the corresponding velocity components are denoted by  $u$  and  $v$ . For the nonlinear solver, in all examples the initial guess (velocity and pressure) is taken as zero, the initial relaxation factor as 0.5, and the relative tolerance as  $10^{-8}$ .

### 4.1. Benchmark problems

Before presenting the rheological fluid models, the scalar shear rate must be defined:

$$\dot{\gamma} := \sqrt{\frac{1}{2} \nabla^s \mathbf{u} : \nabla^s \mathbf{u}}. \quad (33)$$

The generalised Newtonian models are normally given in terms of the dependence between  $\mu$  and  $\dot{\gamma}$ , i.e.,  $\mu = \mu(\nabla^s \mathbf{u}) = \eta(\dot{\gamma})$ . In most of the examples studied here, the chosen material parameters are those of blood. The robustness of the method will be put to test by tackling different models and flow regimes.

#### 4.1.1. Channel flow with power-law fluid

The power-law model is one of the simplest ones used for blood and polymer flows:

$$\eta(\dot{\gamma}) = k\dot{\gamma}^{n-1}. \quad (34)$$

In a straight channel  $\Omega = (0, L) \times (-\frac{H}{2}, \frac{H}{2})$ , it is possible to compute the analytical solution for the hydraulically developed flow:

$$\mathbf{u}(x, y) = \begin{cases} \left( \frac{2n+1}{n+1} \right) \frac{Q}{H} \left( 1 - \left| \frac{2y}{H} \right|^{\frac{n+1}{n}} \right) \\ 0 \end{cases}, \quad (35)$$

$$p(x, y) = \frac{4k}{H} \left[ \left( \frac{2n+1}{n} \right) \frac{Q}{H^2} \right]^n (L - x), \quad (36)$$

where  $Q$  is the volumetric flow rate per unit width. This solution can be used for verifying the order of approximation of the present formulation. The following boundary conditions are considered for the numerical problem: no-slip ( $\mathbf{u} = \mathbf{0}$ ) at the walls ( $y = \pm H/2$ ), the profile from Eq. (35) with  $Q = 100 \text{ mm}^2/\text{s}$  at the inlet ( $x = 0$ ), and the do-nothing condition ( $\tilde{\mathbf{t}} = \mathbf{0}$ ) at the outlet ( $x = L$ ). The material parameters, taken from [14], are:  $\rho = 1050 \text{ kg/m}^3$ ,  $k = 0.035 \text{ Pa}\cdot\text{s}^{0.6}$  and  $n = 0.6$ . As for the geometry,  $L = 3H = 3 \text{ mm}$ . For the convergence study, the coarsest mesh is created by dividing both  $L$  and  $H$  by five, and four levels of uniform refinement are considered. Figure 1 shows the velocity and pressure errors with respect to the mesh size  $h$ . Optimal convergence rates can be verified:

cubic for velocity and quadratic for pressure, in the  $L^2$ -norm. Iterative convergence has also been assessed. The iteration residual is defined as

$$\varepsilon_{n+1} := \frac{|\mathbf{W}^{n+1} - \mathbf{W}^n|}{|\mathbf{W}^{n+1}|}, \quad \text{with } \mathbf{W}^n = \begin{Bmatrix} \underline{\mathbf{u}}^n \\ \underline{p}^n \\ \underline{\tilde{\mu}}^n \end{Bmatrix}. \quad (37)$$

The residual evolution for the coarsest mesh and the finest mesh are depicted in Figure 2, where the expected quadratic convergence can be clearly verified.

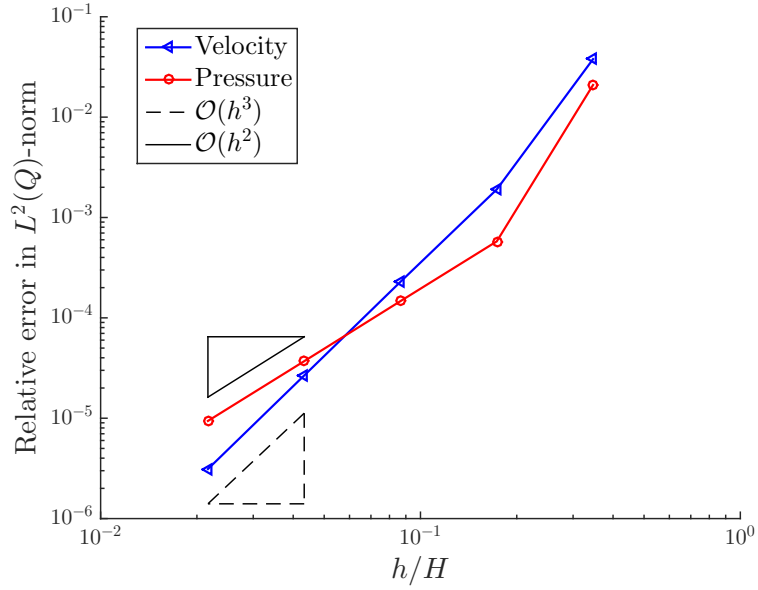


**Figure 1:** Error plot for the power-law channel flow problem.

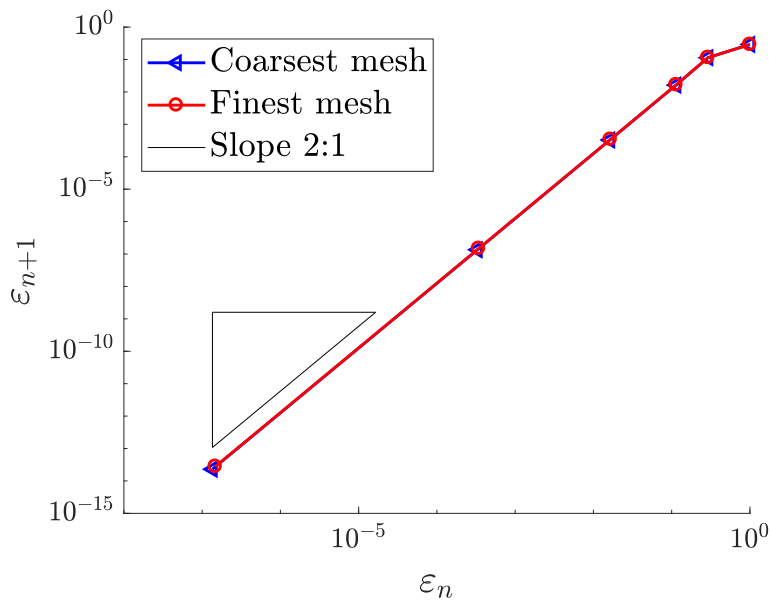


**Figure 2:** Evolution of the iteration residual for the power-law channel flow problem.

#### 4.1.2. Channel flow with Bingham plastic

For this example, a Bingham plastic is considered. Such materials only start flowing when a minimum shear level is reached, but then behave as Newtonian fluids [5]. To avoid the need for tracking yield surfaces, Papanastasiou [15] proposed a smoothed version which fits into the generalised Newtonian framework:

$$\eta(\dot{\gamma}) = \mu_{\infty} + \frac{\tau_0 (1 - e^{-m\dot{\gamma}})}{2\dot{\gamma}}, \quad (38)$$

where  $\mu_{\infty}$  is the Newtonian viscosity,  $\tau_0$  is the yield stress and  $m > 0$  is a regularisation parameter. The exact Bingham model is recovered when  $m \rightarrow \infty$ , but in most applications it is sufficient to consider  $m \geq 10$  s [15]. The analytical expression for the fully developed Bingham flow profile in a straight channel is also known:

$$u = \begin{cases} -\frac{\alpha}{2\mu_{\infty}} \left(\frac{H-D}{2}\right)^2 + \frac{\alpha D^2}{8\mu_{\infty}} \left(1 - \frac{2}{D}|y|\right)^2, & \text{if } \frac{D}{2} < |y| \leq \frac{H}{2}, \\ -\frac{\alpha}{2\mu_{\infty}} \left(\frac{H-D}{2}\right)^2, & \text{if } 0 \leq |y| \leq \frac{D}{2}, \end{cases} \quad (39)$$

where  $D$  is the width of the unyielded region, given by [15]

$$D = -2\frac{\tau_0}{\alpha}, \quad (40)$$

and  $\alpha$  is the pressure gradient in the  $x$  direction. However, when an inflow velocity profile is prescribed instead of a pressure drop, one must first compute  $\alpha$  in terms of  $Q$ . From Eqs. (39) and (40) and the definition of  $Q$ , it is possible to derive a polynomial expression to find  $\alpha$  in terms of the input parameters:

$$\alpha^3 + \frac{3}{H} \left( \frac{4\mu_{\infty}Q}{H^2} + \tau_0 \right) \alpha^2 - 4 \left( \frac{\tau_0}{H} \right)^3 = 0. \quad (41)$$

For this example, a parabolic velocity profile is prescribed at the inlet, and the numerical velocity profile at  $x = L$  is compared to the analytical one. The parameters used are  $\rho = 1050$  kg/m<sup>3</sup>,  $\mu_{\infty} = 3.45$  mPa.s,  $\tau_0 = 0.2$  Pa,  $m = 50$  s and  $L = 10H = 10$  mm. The domain is divided uniformly into  $300 \times 300$  elements. The Reynolds number is defined as

$$\text{Re} := \frac{\bar{u}H}{\nu_{\infty}} = \frac{\rho Q}{\mu_{\infty}}, \quad (42)$$

and three values are considered:  $\text{Re} = 1, 10$  and  $100$ . The comparison between numerical and analytical results, depicted in Figure 3, reveals excellent agreement for all three cases considered. Note that the non-Newtonian behaviour is stronger for low Reynolds numbers, while hardly noticeable for  $\text{Re} = 100$ .

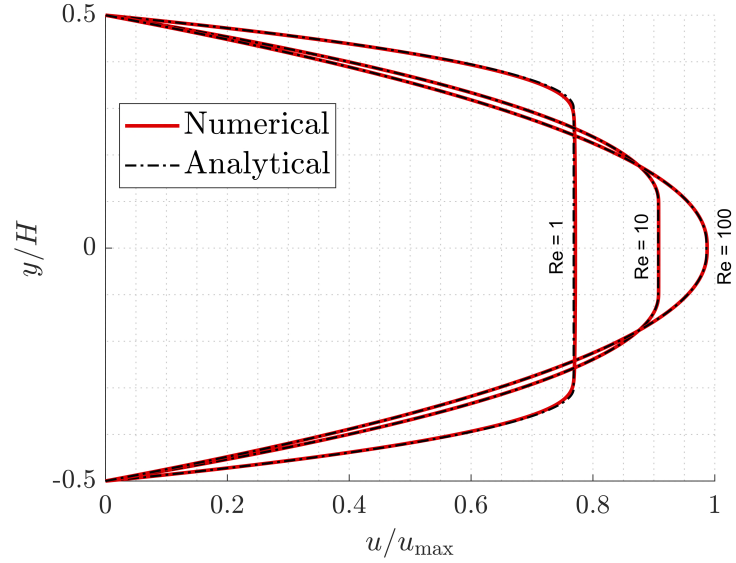


**Figure 3:** Comparison between numerical and analytical solutions for the Bingham channel flow profile.

#### 4.1.3. Backward-facing step with Carreau fluid

Aiming to test the method for more complex flows, the classical backward-facing step benchmark is considered next, with the geometry shown in Figure 4. This problem is particularly interesting for moderately high Reynolds numbers, since a large recirculation area appears (e.g., for  $Re = 100$ ). The Carreau model is chosen for this example:

$$\eta(\dot{\gamma}) = \mu_{\infty} + (\mu_0 - \mu_{\infty}) [1 + (\lambda\dot{\gamma})^2]^{\frac{n-1}{2}}. \quad (43)$$

The material parameters for blood are taken again from [14]:  $\rho = 1050 \text{ kg/m}^3$ ,  $\mu_{\infty} = 3.45 \text{ mPa}\cdot\text{s}$ ,  $\mu_0 = 56 \text{ mPa}\cdot\text{s}$ ,  $n = 0.3568$ ,  $\lambda = 3.313 \text{ s}$ . A parabolic velocity profile is used at the inlet, and the do-nothing boundary condition is considered at the outlet. No-slip is considered on the remainder of the boundary. The inlet height is set as  $H = 1 \text{ mm}$ , and the Reynolds number for this problem is defined as

$$Re := \frac{\bar{u}_{\text{inlet}} H}{\nu_{\infty}} = \frac{\rho Q}{\mu_{\infty}}. \quad (44)$$

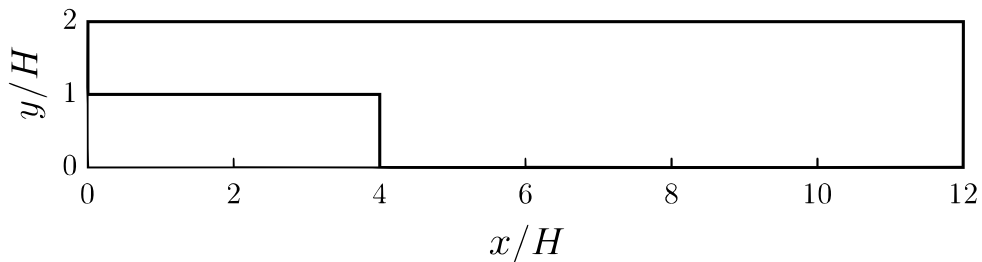


**Figure 4:** L-shaped domain used for the backward-facing step benchmark.

Reference solutions for comparison have been generated with OpenFOAM, which has the Carreau model already built in and uses the Finite Volume Method (FVM). The outlet boundary conditions applied for the finite volume solution are  $p = 0$  and  $\frac{\partial \mathbf{u}}{\partial \mathbf{n}} = \mathbf{0}$ . Three Reynolds numbers are considered:  $Re = 1, 10$  and  $100$ . For the finite element solution, the domain is uniformly divided into square elements of length  $H/50$ . A uniform quadrilateral mesh of sizes  $H/100 \times H/75$  is used for the FVM solution. The velocity profile is sampled at six downstream positions, and the comparison is depicted in Figure 5. It can be observed that the solutions are in very good agreement, and that the present method accurately captures both the complex flow structure (recirculation) and the non-Newtonian effect (profile flattening), all the way up to the boundary.

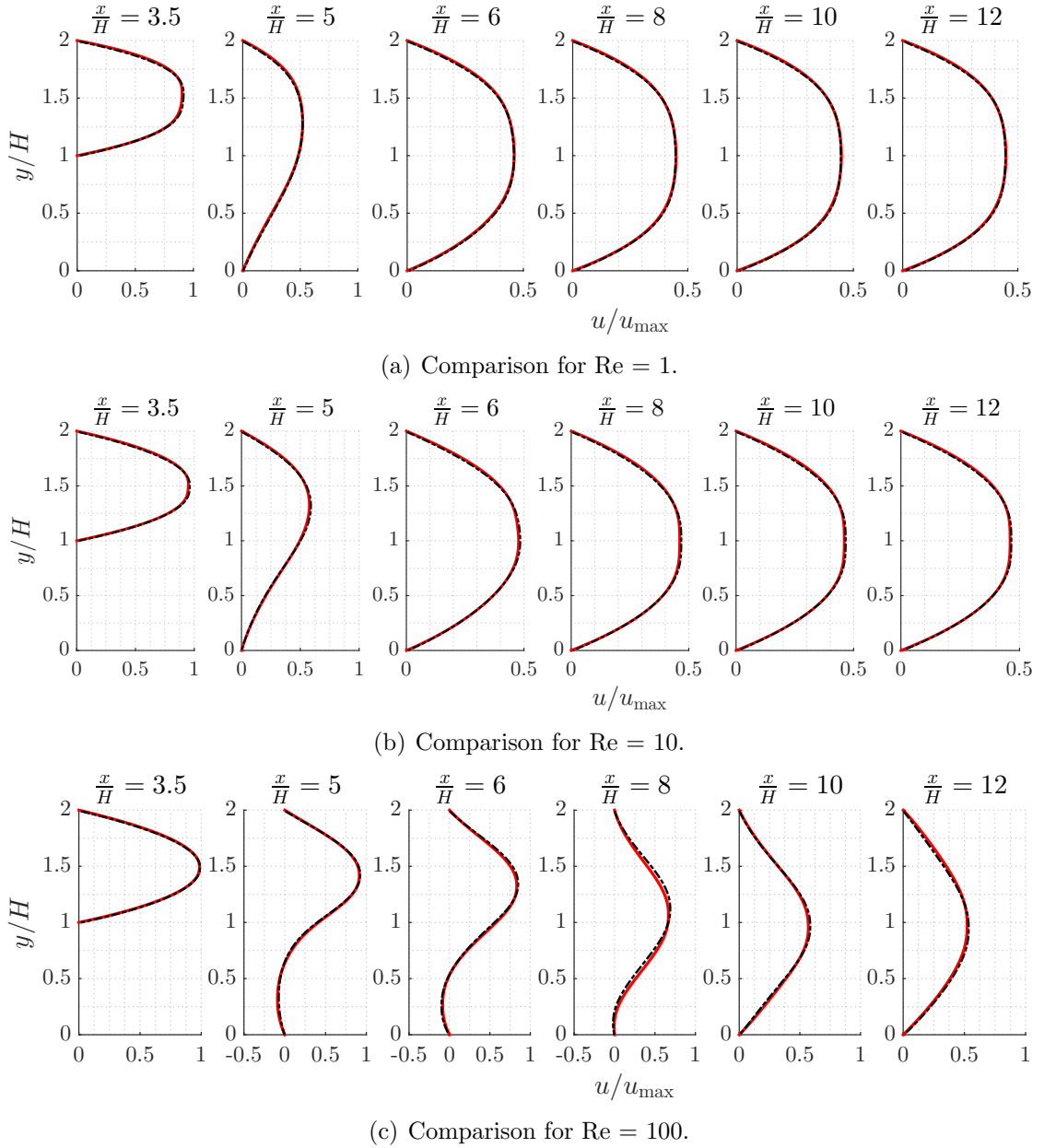


**Figure 5:** Velocity profiles for the backward-facing step problem with Carreau material, for different Reynolds numbers. Solid lines: FEM (new formulation); dotted lines: FVM (OpenFOAM).



#### 4.2. Effect of domain truncation

In this section, the new method is compared to the classical finite element stress-divergence formulation with respect to the effects of domain truncation on the solution. The problem setup and mesh are the same as in Section 4.1.3, using for each formulation its respective do-nothing outlet boundary condition ( $\tilde{\mathbf{t}} = \mathbf{0}$  or  $\mathbf{t} = \mathbf{0}$ ). The comparison is done with respect to the normalised viscosity, namely,

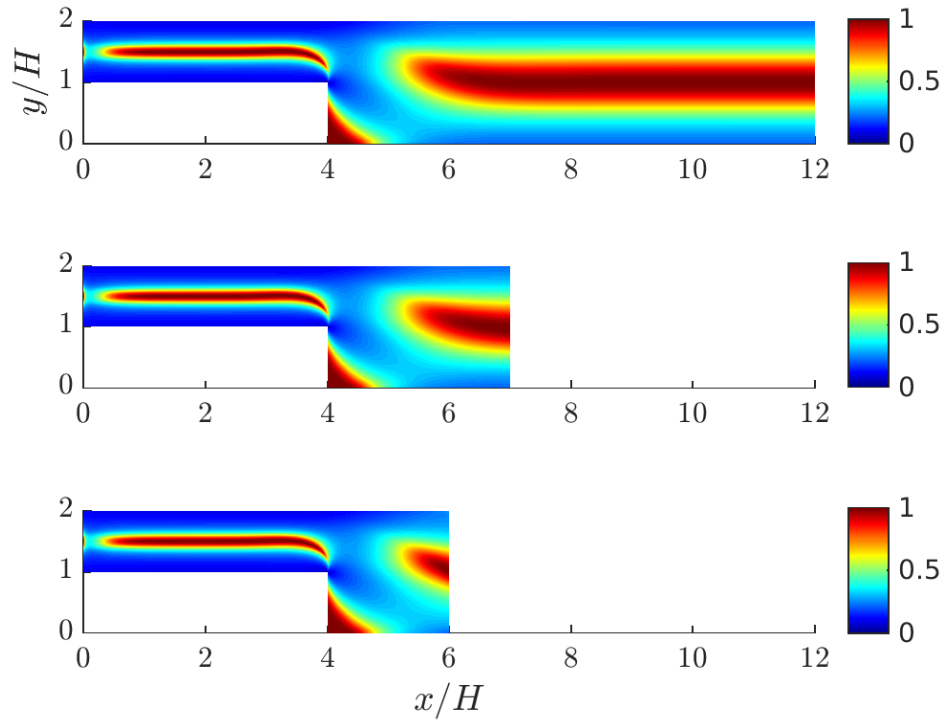
$$\bar{\mu} := \frac{\eta(\dot{\gamma}) - \mu_\infty}{\mu_0 - \mu_\infty}. \quad (45)$$

In the classical formulation, the (post-processed) viscosity field is discontinuous. Therefore, to allow a fair comparison, that viscosity is post-processed using the same continuous  $L^2$ -projection as for the new formulation. Figure 6 depicts the normalised viscosity field computed from both formulations, and considering domains truncated on different positions. Here, the importance of using the right outflow boundary condition is evident. Using the new formulation with  $\tilde{\mathbf{t}} = \mathbf{0}$  yields physically consistent solutions all the way up to the boundary, even when the domain is truncated before the flow is fully developed. On the other hand, the solution produced by the classical approach is highly dependent on the position of the cut, and yields clear unphysical behaviour around the outlet region. If the cut is not placed far enough from the region of interest, great inaccuracy is observed over a large area, as in Figure 6 (bottom).

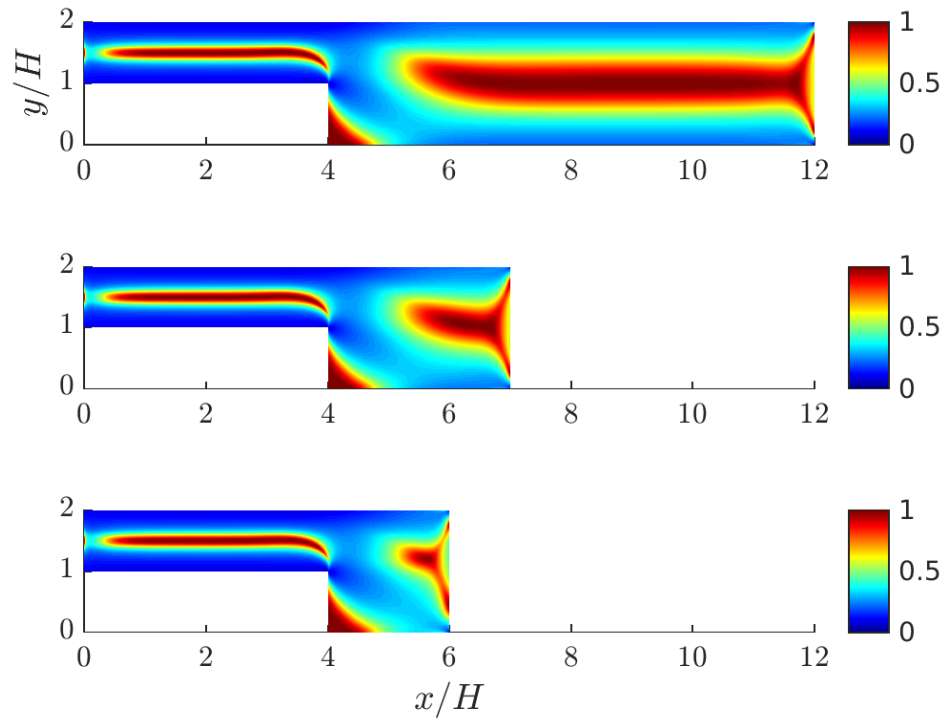
Finally, it is worth noting that in problems with multiple outlets, different mean pressure values  $\bar{p}_i$  can be enforced individually at each outlet  $\Gamma_{N_i}$  by setting  $\tilde{\mathbf{t}}|_{\Gamma_{N_i}} = -\bar{p}_i \mathbf{n}$  [5]. Especially in biomedical applications, various models are available to estimate such mean outflow pressures based on problem-specific features (e.g., Fogliardi et al. [16], Coccarelli et al. [17]).

### 5. Concluding remarks

This work has presented a new finite element formulation for generalised Newtonian fluid flows, aiming to yield appropriate natural boundary conditions for problems set in truncated computational domains. By manipulating the viscous stress tensor appropriately, a formulation can be devised which consists of the Laplace form for the Navier-Stokes equation, plus a contribution from the spatial variation of the viscosity. This novel formulation possesses the same natural boundary conditions as the standard one for Newtonian fluids, which is known to provide physically accurate solutions in truncated domains. For generalised Newtonian fluids, whose viscosity depends on the velocity gradient, a continuous  $L^2$  projection of the viscosity field is employed to avoid higher regularity requirements on the finite element spaces. Comparison with benchmark flow solutions using various non-Newtonian fluid models showcases the accuracy and robustness of the method. Furthermore, comparing the novel formulation and the classical



(a) New formulation.



(b) Classical formulation

**Figure 6:** Viscosity distribution resulting from zero natural outflow condition in truncated domains.

one for non-Newtonian fluids reveals the importance of using appropriate outflow boundary conditions in problems with open outflow boundaries. Although only models with velocity-dependent viscosity have been analysed here, the present formulation requires no modifications for cases where there is also a dependence on the pressure.

## Acknowledgements

The authors acknowledge Graz University of Technology for the financial support of the Lead-project: Mechanics, Modeling and Simulation of Aortic Dissection.

## References

- [1] P.M. Gresho. Some current CFD issues relevant to the incompressible Navier-Stokes equations. *Computer Methods in Applied Mechanics and Engineering*, 87(2-3):201–252, 1991.
- [2] V. John. *Finite element methods for incompressible flow problems*. Springer, 2016.
- [3] J. Donea and A. Huerta. *Finite Element Methods for Flow Problems*. John Wiley & Sons, New York, 2003.
- [4] T. Richter. *Fluid-structure Interactions: Models, Analysis and Finite Elements*. Springer, Heidelberg, 2017.
- [5] G.P. Galdi, R. Rannacher, A.M. Robertson, and S. Turek. *Hemodynamical Flows*, volume 37 of *Oberwolfach Seminars*. Birkhäuser Basel, Basel, 2008.
- [6] A. Masud and J. Kwack. A stabilized mixed finite element method for the incompressible shear-rate dependent non-Newtonian fluids: Variational Multiscale framework and consistent linearization. *Computer Methods in Applied Mechanics and Engineering*, 200(5-8):577–596, 2011.
- [7] S. Serdas, A. Schwarz, J. Schröder, S. Turek, A. Ouazzi, and M. Nickaen. Least-squares finite element methods for the Navier-Stokes equations for generalized Newtonian fluids. *PAMM*, 14(1):623–624, 2014.
- [8] L. John, P. Pustějovská, and O. Steinbach. On the influence of the wall shear stress vector form on hemodynamic indicators. *Computing and Visualization in Science*, 18(4-5):113–122, 2017.
- [9] V.J. Ervin and H. Lee. Numerical approximation of a quasi-Newtonian Stokes flow problem with defective boundary conditions. *SIAM Journal on Numerical Analysis*, 45(5):2120–2140, 2007.
- [10] L. Gesenhues, J.J. Camata, A.M.A. Côrtes, F.A. Rochinha, and A. L.G.A. Coutinho. Finite element simulation of complex dense granular flows using a well-posed regularization of the  $\mu(I)$ -rheology. *Computers & Fluids*, 188:102–113, 2019.

- [11] R. Rannacher. On the Numerical Solution of the Incompressible Navier-Stokes Equations. *ZAMM - Journal of Applied Mathematics and Mechanics / Zeitschrift für Angewandte Mathematik und Mechanik*, 73(9):203–216, 1993.
- [12] J.G. Heywood, R. Rannacher, and S. Turek. Artificial boundaries and flux and pressure conditions for the incompressible Navier-Stokes equations. *International Journal for Numerical Methods in Fluids*, 22(5):325–352, 1996.
- [13] U. Küttler and W.A. Wall. Fixed-point fluid-structure interaction solvers with dynamic relaxation. *Computational Mechanics*, 43(1):61–72, 2008.
- [14] Y.I. Cho and K.R. Kensey. Effects of the non-Newtonian viscosity of blood on flows in a diseased arterial vessel. Part 1: Steady flows. *Biorheology*, 28(3-4):241–62, 1991.
- [15] T.C. Papanastasiou. Flows of materials with yield. *Journal of Rheology*, 31(5):385–404, 1987.
- [16] R. Fogliardi, M. Di Donfrancesco, and R. Burattini. Comparison of linear and non-linear formulations of the three-element windkessel model. *American Journal of Physiology-Heart and Circulatory Physiology*, 271(6):H2661–H2668, dec 1996.
- [17] A. Coccarelli, A. Prakash, and P. Nithiarasu. A novel porous media-based approach to outflow boundary resistances of 1D arterial blood flow models. *Biomechanics and Modeling in Mechanobiology*, 18(4):939–951, aug 2019.